PHYSICAL REVIEW B **95**, 241404(R) (2017)

Resistively detected NMR line shapes in a quasi-one-dimensional electron system

M. H. Fauzi,[1] A. Singha,[2] M. F. Sahdan,[1] M. Takahashi,[1] K. Sato,[1] K. Nagase,[1] B. Muralidharan,[2] and Y. Hirayama[1,3]

[1]*Department of Physics, Tohoku University, Sendai 980-8578, Japan*
[2]*Department of Electrical Engineering, Indian Institute of Technology Bombay, Mumbai 400076, India*
[3]*Center for Spintronics Research Network, Tohoku University, Sendai 980-8577, Japan*

(Received 9 March 2017; published 9 June 2017)

We observe variation in the resistively detected nuclear magnetic resonance (RDNMR) line shapes in quantum Hall breakdown. The breakdown occurs locally in a gate-defined quantum point contact (QPC) region. Of particular interest is the observation of a dispersive line shape occurring when the bulk two-dimensional electron gas (2DEG) set to $\nu_b = 2$ and the QPC filling factor to the vicinity of $\nu_{QPC} = 1$, strikingly resemble the dispersive line shape observed on a 2D quantum Hall state. This previously unobserved line shape in a QPC points to a simultaneous occurrence of two hyperfine-mediated spin flip-flop processes within the QPC. Those events give rise to two different sets of nuclei polarized in the opposite direction and positioned at a separate region with different degrees of electronic spin polarization.

DOI: 10.1103/PhysRevB.95.241404

The recent advent in NMR technique through a resistive detection, resistively detected nuclear magnetic resonance (RDNMR), has made it possible to study various spin physics in a two-dimensional (2D) quantum Hall system [1–7], and a quasi-one-dimensional channel [8,9]. Despite the success achieved, a certain aspect related to the origin of the RDNMR line-shape variations noted experimentally in continuous wave (cw) mode is still poorly understood. One of them involved the puzzling observation of a dispersive line shape in the quantum Hall state, a resistance dip followed by a resistance peak resonance line with increasing radio frequency [10]. It is first reported by Desrat *et al.* [11] in the vicinity of $\nu_b = 1$ and has been confirmed in a number of follow-up papers [7,12–17]. Similar dispersivelike line shape has been observed as well in the vicinity of $\nu_b = 2/9$ [18], $\nu_b = 2/3$, $\nu_b = 1/3$ [19], and at $\nu_b = 2$ Landau level crossing [20]. A number of appealing explanations have been put forward, but none of them provides a comprehensive explanation. Part of the reason why it is still difficult to unravel its physical origin is that we do not yet have a mature level of understanding about many-body 2D electronic states at the first Landau level, let alone their coupling to the nuclear spin. Thus, it would be highly desirable to study the line-shape variations in a platform where one can avoid such complexity.

In this Rapid Communication, we resort to a quasi-one-dimensional system in a gate-defined quantum point contact (QPC) to study various possible line shapes including the dispersive line shape noted experimentally in cw mode. Unlike on the 2D system, the mechanism for generation and resistive detection of nuclear spin polarization is tractable, allowing conveniently a direct interpretation of the observed line shapes.

Generation and detection of nuclear spin polarization are achieved by setting the filling factor in the bulk two-dimensional electron gas (2DEG) to $\nu_b = 2$ and $\nu_{QPC} = 1$ in the QPC [21–30]. Figures 1(a) and 1(b) schematically display how the nuclear polarization affects the transmission probability through the potential barrier of the QPC. For $\nu_{QPC} < 1$ (the down-spin channel $T_\downarrow$ does not affect the transport), the up-spin channel $T_\uparrow$ sees an increase (decrease) in the barrier potential in the presence of positive (negative) nuclear polarization, where positive (negative) means nuclear polarization is parallel (opposite) to the external magnetic field. Consequently, the transmission probability of the up-spin channel is reduced (enhanced). Therefore, the transmission is modified by a dynamic nuclear polarization (DNP) under a steady state where nuclear spins diffuse from the polarized regions to the center of the QPC. At sufficiently high current densities, there are two possible tractable DNPs by hyperfine-mediated interedge spin-flip scattering within the lowest Landau level, namely, forward and backward spin-flip scatterings [21,22,31]. The first (second) one involves a spin-flip scattering from the forward propagating up-spin (down-spin) channel to the forward (backward) propagating down-spin (up-spin) channel, which in turn produces the positive (negative) nuclear polarization through the spin flip-flop process. On sweeping the rf field after the polarization reaches a steady state, those two different sets of nuclear polarization would leave a different trace in the RDNMR signal; with the positive (negative) one resulting in a resistance dip (peak). Here we demonstrate that under certain electronic states in the QPC, those two sets of nuclei can be generated simultaneously in a separate region within the QPC. Since they experience different degrees of electron spin polarization, one can observe a combination of a resistance dip and peak resonance line in the RDNMR spectrum, namely, dispersive line shape.

Our studies are carried out on a 20-nm-wide doped GaAs quantum well with the 2DEG located 165 nm beneath the surface. The wafer is photolithographically carved into a 30-μm-wide and 100-μm-long Hall bar geometry. The low temperature electron mobility is 84.5 m^2/V s at an electron density of 1.0×10^{15} m^{-2}. A single QPC defined by triple Schottky gates is patterned on top of the Hall bar by Ti/Au evaporation. The bulk 2DEG density n can be tuned by applying back-gate voltage (V_{BG}) to Si-doped GaAs substrate. It enables us to control the filling factor of interest in the bulk 2DEG $\nu = \frac{h}{eB} n$ with back gate V_{BG} and magnetic field B. The samples are mounted inside a single-shot cryogenic-free ^{3}He refrigerator with a temperature of 300 mK. A six-turn rf coil wrapped the sample to be able to apply an oscillating magnetic field in the plane of the 2DEG. Throughout this study,

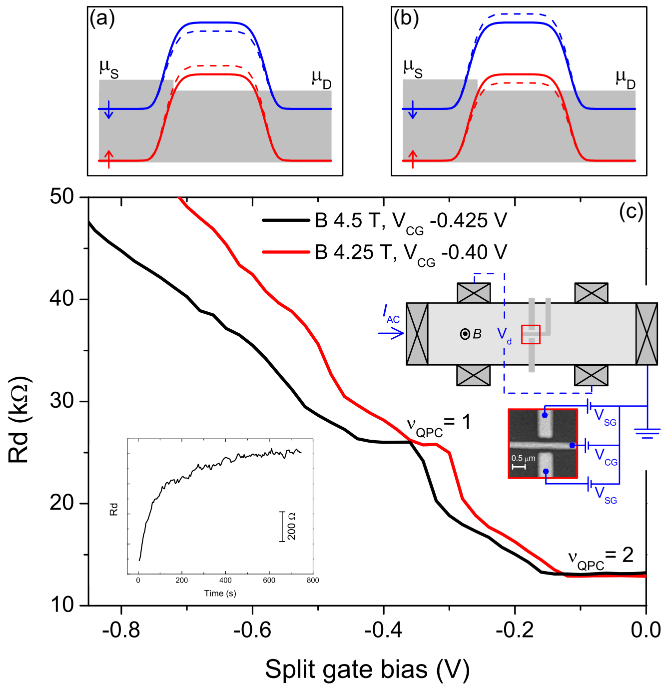

FIG. 1. (a),(b) Schematic of potential barrier seen by up-spin and down-spin electrons without (solid line) and with (dashed line) the presence of positive and negative nuclear polarization, respectively. The chemical potential window sits at $\nu_{QPC} < 1$, so that only the up-spin channel affects the transport. (c) Differential diagonal resistance $R_d \equiv dV_d/dI_{AC}$ curve versus split gate bias voltage (V_{SG}) at a field of 4.5 (black) and 4.25 T (red). The left and right split gates are biased equally. The center gate voltage V_{CG} is fixed to -0.425 and -0.4 V, respectively. The upper inset displays a schematic drawing of the device. Cross marks represent Ohmic contact pads. Triple Schottky gates deposited on top of the Hall bar defined a quantum point contact (see the scanning electron microscopy image). The lithographic gap (width) between (of) a pair of split gates is 600 (500) nm. An extra gate (center gate) with lithographic width of 200 nm is deposited in between the split gates. An excitation current $I_{ac} = 1$ nA with $f = 13.7$ Hz is applied to the device for transport measurement. The lower inset shows typical R_d time trace during current-induced dynamic nuclear polarization with $I_{ac} = 10$ nA.

the amplitude of rf power delivered to the top of the cryostat is fixed to -30 dBm (unless specified otherwise).

Figure 1(c) displays two sets of diagonal resistance traces as a function of split gate bias voltage across the QPC measured at a field of 4.5 (black line) and 4.25 (red line) T. The center gate is fixed to $V_{CG} = -0.425$ V and $V_{CG} = -0.4$ V, respectively [32]. We start with fully filled first Landau level in the bulk 2DEG ($\nu_b = 2$), where both the up-spin and down-spin electrons are available for transmission. Applying negative voltage on the split gates allows us to selectively transmit the up-spin channel through the constriction and reflect the down-spin channel. The nuclear spin is dynamically polarized by applying $I_{ac} = 10$ nA at a selected operating point along the diagonal resistance trace on both sides of the $\nu_{QPC} = 1$ plateau. Typically, the resistance increases exponentially and reaches a point of saturation on the time scale of a few hundred seconds with the characteristic exponential rise time of about 150 s (see the lower inset of Fig. 1); a similar time scale characteristic is reported previously on other QPC structures [28]. Once the resistance saturates, the rf is swept across the Larmor frequency of ^{75}As nuclei while measuring its resistance. The rf sweep rate is set to 100 Hz/s [33].

We observe variation in the RDNMR line-shape spectra on both flanks of the $\nu_{QPC} = 1$ plateau as displayed in Figs. 2 and 3. Let us start with the RDNMR spectra for the $\nu_{QPC} < 1$ case observed at a field of 4.5 T shown in Fig. 2(a), measured from $V_{SG} = -0.41$ up to $V_{SG} = -0.7$ V. For ease of comparison, we plot the resistance variation ΔR_d with respect to the off-resonance resistance at $f = 33$ MHz. The salient feature appears in a narrow portion of the split gate bias voltage region, $-0.50 \leqslant V_{SG} \leqslant -0.41$ V, very close to the $\nu_{QPC} = 1$ plateau. The spectra have a curious dispersive line shape, and strikingly resemble the dispersive line shape previously observed in a number of reports on a 2D quantum Hall system in the vicinity of $\nu_b = 1$ [7,11–17]. The line shape we observe in our system is found to be highly sensitive to the rf power such that the resistance peak resonance line vanishes at a relatively high rf power of -15 dBm [34].

The corresponding signal amplitude normalized to the off-resonance resistance $|\Delta R_d|/R_d$ is displayed in Fig. 2(b). All the signal amplitude observed here falls below 1%, similar to the previous reports in Refs. [28,29]. Starting from the observable signal closest to the plateau $V_{SG} = -0.41$ V, the dip amplitude shows a sharp upturn and reaches a maximum value at $V_{SG} = -0.44$ V. It is then followed by a downturn and takes on a minimum value at $V_{SG} = -0.50$ V, precisely at the transition between dispersive-to-single line shape. The peak amplitude has a smaller amplitude than the dip amplitude and shows a monotonic decrease from $V_{SG} = -0.42$ V and eventually vanishes at $V_{SG} = -0.51$ V. The spectrum evolves into an expected single dip line shape for $V_{SG} \leqslant -0.51$ V with the signal amplitude gradually increasing. It can be partially explained by an increase in the current density locally in the constriction. Altogether, the fact that the line shapes, signal amplitudes, as well as resonance point vary with the split gate bias voltage constitute firm evidence that the nuclei is polarized locally in the QPC.

In Figs. 2(c) and 2(d) we plot the raw RDNMR spectra at the two most extreme cases, $V_{SG} = -0.70$ and $V_{SG} = -0.41$, respectively. In order to extract the Knight shift for each spectrum, here we plot in Fig. 2(d) (red dots) the reference signal taken close to $\nu_b = 2$ with nearly zero Knight shift. The spectrum is fitted with a Gaussian function [27], centered at 33.057 MHz and FWHM of 8.8 kHz (red line). Note that the long tail in the higher radio frequency side in the reference spectrum is nothing but reflects a long T1 time [35]. Comparing with the reference signal, the observed spectrum at $V_{SG} = -0.70$ V is only Knight shifted by about 8 kHz, a reasonable value for the spectrum very far from the plateau at a field of 4.5 T. The dip frequency in the dispersive line shape at $V_{SG} = -0.41$ V gives the largest observable shift by about 18 kHz. Interestingly, its peak frequency appears to be substantially unshifted as it is aligned reasonably well with the reference resonance point. RDNMR measurement performed at a smaller field of 4.25 T reveals similar line-shape patterns [36].

Figure 2(e) displays the dip and peak resonance line points extracted from the split gate bias voltage segment

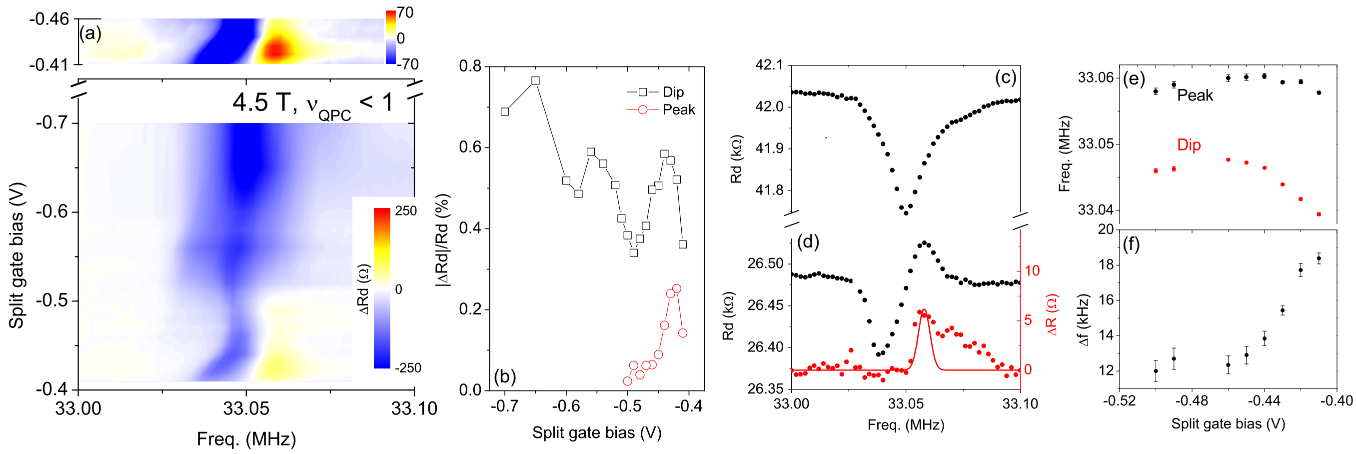

FIG. 2. (a) The lower plot shows a 2D color map of ^{75}As RDNMR traces at the upper flank of the $\nu_{QPC} = 1$ plateau, $-0.70 \leqslant V_{SG} \leqslant -0.41$ V, measured at 4.5 T. The background resistance has been subtracted from the spectrum. The upper plot shows the blown-up spectra in between $-0.46 \leqslant V_{SG} \leqslant -0.41$ V to accentuate the dispersive structure. (b) The RDNMR amplitude percentage vs split gate normalized to the off-resonance resistance, $|\Delta Rd|/Rd$, extracted from panel (a). (c),(d) Raw RDNMR data sliced at the $V_{SG} = -0.7$ and $V_{SG} = -0.41$ V, respectively. RDNMR in red dots superimposed in panel (d) measured very close to the bulk 2DEG $\nu = 2$ plateau, served as a reference signal with almost zero Knight shift. The signal is obtained by applying $I_{AC} = 100$ nA. The red line is a Gaussian fit to the spectrum with the FWHM of 8.8 kHz. (e) The position of peak resonance frequency (black dots) and dip resonance frequency (red dots) extracted from panel (a) for $-0.50 \leqslant V_{SG} \leqslant -0.41$ V. (f) The peak-to-dip resonance frequency separation Δf extracted from panel (e). All the spectra measured with $I_{ac} = 10$ nA (except the ref. signal) and rf power is -30 dBm.

between -0.41 and -0.50 V, where the dispersive line shape is observed. The peak resonance line lies at the resonance reference point with very small variation throughout the range, substantially not Knight shifted. On the other hand, the dip resonance line is upshifted in a linear fashion up to $V_{SG} = -0.46$ V and then followed by a slight downshift. The resulting Δf values extracted from panel (e) are plotted in Fig. 2(f). The Δf value continuously drops down to 12 kHz in an obviously linear fashion up until $V_{SG} = -0.46$ V from its initial value of 18.3 kHz at $V_{SG} = -0.41$ V, bearing a similarity to the $\Delta f - B$ plot around $\nu_b = 1$ observed on the 2D system [16]. The value remains constant at about 12 kHz throughout the remaining split gate values, an indication that the electronic state in the QPC does not change significantly. A similar trend is observed as well for a field of 4.25 T [37].

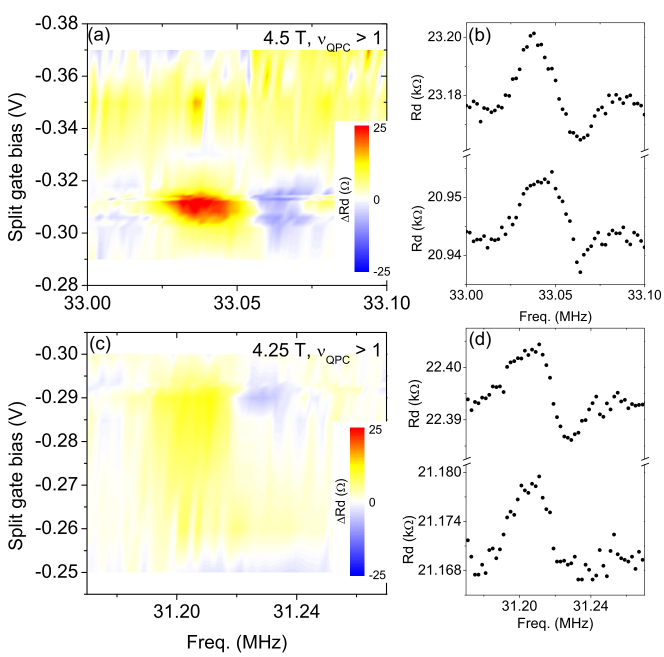

FIG. 3. (a) 2D color map of ^{75}As RDNMR traces at the lower flank of the $\nu_{QPC} = 1$ plateau ($\nu_{QPC} > 1$) measured at a field of 4.5 T. (b) Raw RDNMR traces sliced at $V_{SG} = -0.313$ (upper) and $V_{SG} = -0.302$ (lower) V, respectively. (c) 2D color map of ^{75}As RDNMR traces at the lower flank of the $\nu_{QPC} = 1$ plateau ($\nu_{QPC} > 1$) measured at a field of 4.25 T. (d) Raw RDNMR traces sliced at $V_{SG} = -0.29$ (upper) and $V_{SG} = -0.285$ (lower) V, respectively.

We now move on to discuss the RDNMR taken at the opposite side of the plateau ($\nu_{QPC} > 1$) as shown in Fig. 3. The data show a similar line-shape trend, but with inverted signal and much smaller amplitude than its counterpart. At a field of 4.5 T displayed in Fig. 3(a), the RDNMR signal is visible only in a confined split gate bias range, $-0.32 \leqslant V_{SG} \leqslant -0.30$ V. The spectra measured very close to the plateau are hindered by a large resistance fluctuation in particular at the point where the diagonal resistance abruptly changes. Nevertheless, one can verify the existence of the inverted dispersive line shape for $\nu_{QPC} > 1$ [see the line cuts at $V_{SG} = -0.313$ and $V_{SG} = -0.302$ V in Fig. 3(b) for better visual]. The RDNMR signal measured at a field of 4.25 T displayed in Fig. 3(c) has less resistance fluctuation and hence offers better signal-to-noise ratio. The inverted dispersive line shape appears at $V_{SG} = -0.29$ V [upper Fig. 3(d)] and turns into a resistance peak line shape at $V_{SG} = -0.285$ V [lower Fig. 3(d)]. In contrast to the case for $\nu_{QPC} < 1$ where the RDNMR signal is observed in a wide range of split gate bias voltages, the signal observed here vanishes very quickly far from the $\nu_{QPC} = 1$ plateau region. Recall that the hyperfine-mediated spin flip-flop process relies on the spatial overlap between the up-spin and down-spin channels [21]. Thus, the absence

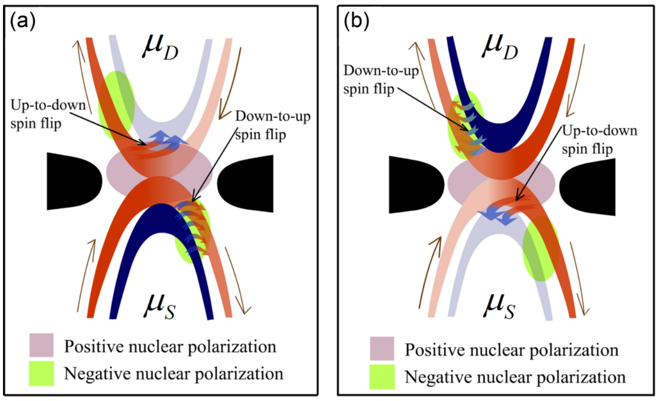

FIG. 4. (a) Schematics of Landauer-Büttiker edge channel with forward (up-to-down spin flip) and backward (down-to-up spin flip) hyperfine-mediated spin-flip scatterings occurring at filling factors slightly smaller than $\nu_{\rm QPC} \approx 1$ during the first half-clock alternating current cycle ($\mu_S > \mu_D$) and (b) during the second half-clock alternating current cycle ($\mu_S < \mu_D$). Lighter edges indicate an empty channel while darker edges indicate a filled channel. The drain is held at ground ($\mu_D = 0$) while the source chemical potential $\mu_S = 0$ oscillates at a frequency of 13.7 Hz.

of a RDNMR signal indicates that the critical current for breakdown is higher than for $\nu_{\rm QPC} < 1$ since the channel is opened wider [38].

The results presented in Figs. 2 and 3 provide important insights into the mechanisms leading to the dispersive line shape observed in the vicinity of the $\nu_{\rm QPC} = 1$ plateau. Figure 4 displays all possible hyperfine-mediated spin-flip scattering events where the QPC filling factor is tuned slightly less than 1 for two different alternating current cycles. The forward and backward spin-flip scattering could occur simultaneously within the QPC. The forward scattering occurs at the central region of the QPC where the degree of electron spin polarization is finite, not zero. On the other hand, the backward spin-flip scattering occurs slightly outside the central region where the electron spin polarization is zero. These two scattering events occur in spatially separated regions and give rise to localized nuclear polarization in the opposite directions. On sweeping of the rf with increasing frequency, the positive nuclear polarization is destroyed first due to Knight shift. It results in an increase in the transmissivity of the up-spin channel. On further sweeping the rf, the positive nuclear polarization starts to build up and negative nuclear polarization is destroyed. This results in a decrease in the transmissivity of the up-spin channel. The backward spin-flip scattering is highly suppressed when the QPC filling factor is further tuned to $\nu_{\rm QPC} < 1$, leaving only positive nuclear polarization buildup at the central region of the QPC. The RDNMR spectrum switches from dispersivelike to dip resonance line shape. In this scenario, the Knight shift at the central region is determined by $K_S \propto (n_\uparrow - n_\downarrow) \propto (T_\uparrow - T_\downarrow)$, where $n_\uparrow(n_\downarrow)$ and $T_\uparrow(T_\downarrow)$ are up(down)-spin electron density and up(down)-spin transmission probability, respectively. The Knight shift reaches a maximum value when the up-spin channel is completely transmitted ($T_\uparrow = 1$) while the down-spin channel is completely reflected ($T_\downarrow = 0$). It decreases with reduction of $T_\uparrow$, agreeing well with the experimental data shown in Fig. 2(e).

For $\nu_{\rm QPC} > 1$ case, a similar scenario happens. However, the Overhauser field from the polarized nuclei now affects the transmission of the down-spin channel while the fully transmitted up-spin channel is left unaffected. The nuclear polarization influences the transmissivity of the down-spin channel in an opposite way than that of the up-spin channel. This is the reason why the RDNMR spectrum gets inverted, as experimentally confirmed in Fig. 3 and noted in Ref. [29].

To summarize, here we observe four variations of the RDNMR line shapes in a gate-defined QPC. Of particular interest is the emergence of the dispersive line shape in the RDNMR signal when the bulk filling factor is set to $\nu_{\rm b} = 2$ and the QPC filling factor to the vicinity of the $\nu_{\rm QPC} = 1$ plateau. It can be accounted for by considering the simultaneous occurrence of two hyperfine-mediated spin-flip scattering events due to current-induced dynamic nuclear polarization. These phenomena give rise to localized regions with opposite nuclear polarization in the QPC. Although both of them are in contact with electrons in the QPC, they polarize in a region with different degrees of electron spin polarization. Our experimental results further cemented the idea that the observation of the dispersive line shapes on the 2D system, in particular around $\nu_{\rm b} = 1$, should reflect the nuclear spin interaction with two electronic subsystems as suggested by the authors in Refs. [7,16].

We would like to thank K. Muraki of NTT Basic Research Laboratories for supplying high quality wafers for this study. We thank K. Hashimoto, K. Akiba, T. Aono, T. Tomimatsu, B. Friess, A. Micholic, and D. G. Austing for helpful discussions and/or technical assistance. M.H.F. and Y.H. acknowledge support from Multi-Dimensional program, Tohoku University. A.S., M.T., K.N., and Y.H. acknowledge support from Graduate Program in Spintronics, Tohoku University. B.M. and Y.H. acknowledge support from WPI-AIMR, Tohoku University. Y.H. acknowledges financial support from KAKENHI Grants No. 26287059 and No. 15H05867. B.M. and A.S. acknowledge funding from the Department of Science and Technology, India under the Science and Engineering Board (SERB) Grant No. SERB/F/3370/2013-2014.

[1] N. Kumada, K. Muraki, and Y. Hirayama, Phys. Rev. Lett. **99**, 076805 (2007).
[2] X. C. Zhang, G. D. Scott, and H. W. Jiang, Phys. Rev. Lett. **98**, 246802 (2007).
[3] M. Stern, B. A. Piot, Y. Vardi, V. Umansky, P. Plochocka, D. K. Maude, and I. Bar-Joseph, Phys. Rev. Lett. **108**, 066810 (2012).
[4] L. Tiemann, G. Gamez, N. Kumada, and K. Muraki, Science **335**, 828 (2012).
[5] B. Friess, V. Umansky, L. Tiemann, K. von Klitzing, and J. H. Smet, Phys. Rev. Lett. **113**, 076803 (2014).
[6] L. Tiemann, T. D. Rhone, N. Shibata, and K. Muraki, Nat. Phys. **10**, 648 (2014).

[7] B. A. Piot, W. Desrat, D. K. Maude, D. Kazazis, A. Cavanna, and U. Gennser, Phys. Rev. Lett. **116**, 106801 (2016).

[8] A. Kou, D. T. McClure, C. M. Marcus, L. N. Pfeiffer, and K. W. West, Phys. Rev. Lett. **105**, 056804 (2010).

[9] M. Kawamura, K. Ono, P. Stano, K. Kono, and T. Aono, Phys. Rev. Lett. **115**, 036601 (2015).

[10] G. Gervais, Resistively detected NMR in GaAs/AlGaAs, in *Electron Spin Resonance and Related Phenomena in Low-Dimensional Structures*, edited by M. Fanciulli (Springer, Berlin/Heidelberg, 2009), pp. 35–50.

[11] W. Desrat, D. K. Maude, M. Potemski, J. C. Portal, Z. R. Wasilewski, and G. Hill, Phys. Rev. Lett. **88**, 256807 (2002).

[12] L. A. Tracy, J. P. Eisenstein, L. N. Pfeiffer, and K. W. West, Phys. Rev. B **73**, 121306 (2006).

[13] K. Kodera, H. Takado, A. Endo, S. Katsumoto, and Y. Iye, Phys. Status Solidi C **3**, 4380 (2006).

[14] C. R. Dean, B. A. Piot, G. Gervais, L. N. Pfeiffer, and K. W. West, Phys. Rev. B **80**, 153301 (2009).

[15] C. R. Bowers, G. M. Gusev, J. Jaroszynski, J. L. Reno, and J. A. Simmons, Phys. Rev. B **81**, 073301 (2010).

[16] W. Desrat, B. A. Piot, S. Krämer, D. K. Maude, Z. R. Wasilewski, M. Henini, and R. Airey, Phys. Rev. B **88**, 241306 (2013).

[17] W. Desrat, B. A. Piot, D. K. Maude, Z. R. Wasilewski, M. Henini, and R. Airey, J. Phys.: Condens. Matter **27**, 275801 (2015).

[18] G. Gervais, H. L. Stormer, D. C. Tsui, L. W. Engel, P. L. Kuhns, W. G. Moulton, A. P. Reyes, L. N. Pfeiffer, K. W. Baldwin, and K. W. West, Phys. Rev. B **72**, 041310 (2005).

[19] O. Stern, N. Freytag, A. Fay, W. Dietsche, J. H. Smet, K. von Klitzing, D. Schuh, and W. Wegscheider, Phys. Rev. B **70**, 075318 (2004).

[20] K. F. Yang, H. W. Liu, K. Nagase, T. D. Mishima, M. B. Santos, and Y. Hirayama, Appl. Phys. Lett. **98**, 142109 (2011).

[21] K. R. Wald, L. P. Kouwenhoven, P. L. McEuen, N. C. van der Vaart, and C. T. Foxon, Phys. Rev. Lett. **73**, 1011 (1994).

[22] D. C. Dixon, K. R. Wald, P. L. McEuen, and M. R. Melloch, Phys. Rev. B **56**, 4743 (1997).

[23] T. Machida, T. Yamazaki, and S. Komiyama, Appl. Phys. Lett. **80**, 4178 (2002).

[24] A. Würtz, R. Wildfeuer, A. Lorke, E. V. Deviatov, and V. T. Dolgopolov, Phys. Rev. B **65**, 075303 (2002).

[25] E. V. Deviatov, A. Würtz, A. Lorke, M. Yu. Melnikov, V. T. Dolgopolov, D. Reuter, and A. D. Wieck, Phys. Rev. B **69**, 115330 (2004).

[26] A. Würtz, T. Müller, A. Lorke, D. Reuter, and A. D. Wieck, Phys. Rev. Lett. **95**, 056802 (2005).

[27] S. Masubuchi, K. Hamaya, and T. Machida, Appl. Phys. Lett. **89**, 062108 (2006).

[28] A. Córcoles, C. J. B. Ford, M. Pepper, G. A. C. Jones, H. E. Beere, and D. A. Ritchie, Phys. Rev. B **80**, 115326 (2009).

[29] Z. K. Keane, M. C. Godfrey, J. C. H. Chen, S. Fricke, O. Klochan, A. M. Burke, A. P. Micolich, H. E. Beere, D. A. Ritchie, K. V. Trunov, D. Reuter, A. D. Wieck, and A. R. Hamilton, Nano Lett. **11**, 3147 (2011).

[30] K. Chida, M. Hashisaka, Y. Yamauchi, S. Nakamura, T. Arakawa, T. Machida, K. Kobayashi, and T. Ono, Phys. Rev. B **85**, 041309 (2012).

[31] A. Singha, M. H. Fauzi, Y. Hirayama, and B. Muralidharan, Phys. Rev. B **95**, 115416 (2017).

[32] Tuning the center gate bias to -0.425 (-0.4) V for a field of 4.5 (4.25) T, we effectively make the channel wide so that the resistance increases gradually for $\nu_{\mathrm{QPC}} < 1$. This gradual change in the diagonal resistance makes systematic RDNMR measurement possible for $\nu_{\mathrm{QPC}} < 1$.

[33] See Supplemental Material at http://link.aps.org/supplemental/10.1103/PhysRevB.95.241404 for rf sweep rate dependence characteristics.

[34] See Supplemental Material at http://link.aps.org/supplemental/10.1103/PhysRevB.95.241404 for rf power dependence.

[35] K. Hashimoto, K. Muraki, T. Saku, and Y. Hirayama, Phys. Rev. Lett. **88**, 176601 (2002).

[36] See Supplemental Material at http://link.aps.org/supplemental/10.1103/PhysRevB.95.241404 for $\nu_{\mathrm{QPC}} < 1$ RDNMR line shape at a field of 4.25 T.

[37] See Supplemental Material at http://link.aps.org/supplemental/10.1103/PhysRevB.95.241404 for Δf trend for $\nu_{\mathrm{QPC}} < 1$ at a field of 4.25 T.

[38] S. W. Hwang, D. C. Tsui, and M. Shayegan, Phys. Rev. B **48**, 8161 (1993).